Molecular switch architecture determines response properties of signaling pathways

Khem Raj Ghusinga[a,b,c], Roger D. Jones[d], Alan M. Jones[a,b,1], and Timothy C. Elston[b,c,1]

[a]Department of Biology, University of North Carolina at Chapel Hill, Chapel Hill, NC 27599; [b]Department of Pharmacology, University of North Carolina at Chapel Hill, Chapel Hill, NC 27599; [c]Computational Medicine Program, University of North Carolina at Chapel Hill, Chapel Hill, NC 27599; and [d]Center for Complex Systems and Enterprises, Stevens Institute of Technology, Hoboken, NJ 07030

Edited by Jeff Hasty, University of California San Diego, La Jolla, CA, and accepted by Editorial Board Member James J. Collins January 25, 2021 (received for review June 30, 2020)

Many intracellular signaling pathways are composed of molecular switches, proteins that transition between two states—*on* and *off*. Typically, signaling is initiated when an external stimulus activates its cognate receptor that, in turn, causes downstream switches to transition from *off* to *on* using one of the following mechanisms: activation, in which the transition rate from the *off* state to the *on* state increases; derepression, in which the transition rate from the *on* state to the *off* state decreases; and concerted, in which activation and derepression operate simultaneously. We use mathematical modeling to compare these signaling mechanisms in terms of their dose–response curves, response times, and abilities to process upstream fluctuations. Our analysis elucidates several operating principles for molecular switches. First, activation increases the sensitivity of the pathway, whereas derepression decreases sensitivity. Second, activation generates response times that decrease with signal strength, whereas derepression causes response times to increase with signal strength. These opposing features allow the concerted mechanism to not only show dose–response alignment, but also to decouple the response time from stimulus strength. However, these potentially beneficial properties come at the expense of increased susceptibility to upstream fluctuations. We demonstrate that these operating principles also hold when the models are extended to include additional features, such as receptor removal, kinetic proofreading, and cascades of switches. In total, we show how the architecture of molecular switches govern their response properties. We also discuss the biological implications of our findings.

signaling pathways | activation | derepression | dose–response | noise

Several molecules involved in intracellular signaling pathways act as molecular switches. These are proteins that can be temporarily modified to transition between two conformations, one corresponding to an *on* (active) state and another to an *off* (inactive) state. Two prominent examples of such switches are proteins that are modified by phosphorylation and dephosphorylation and GTPases that bind nucleotides. For phosphorylation–dephosphorylation cycles, it is common for the covalent addition of a phosphate by a kinase to cause activation of the modified protein. A phosphatase removes the phosphate to turn the protein *off*. In the GTPase cycle, the protein is *on* when bound to guanosine triphosphate (GTP) and *off* when bound to guanosine diphosphate (GDP). The transition from the GDP-bound state to the GTP-bound state requires nucleotide exchange, whereas the transition from the GTP-bound to the GDP-bound state is achieved via hydrolysis of the γ phosphate on GTP. The basal rates of nucleotide exchange and hydrolysis are often small. These reaction rates are increased severalfold by Guanine Exchange Factors (GEFs) and GTPase Accelerating Proteins (GAPs), respectively (1, 2).

A signaling pathway is often initiated upon recognition of a stimulus by its cognate receptor, which then activates a downstream switch. In principle, a switch may be turned *on* by three mechanisms: (a) *activation*, by increasing the transition rate from the *off* state to the *on* state; (b) *derepression*, by decreasing the transition rate from the *on* state to the *off* state; and (c) *concerted* activation and derepression. Examples of these three mechanisms are found in the GTPase cycles in different organisms. In animals, signaling through many pathways is initiated by G-protein-coupled receptors (GPCRs) that respond to a diverse set of external stimuli. These receptors act as GEFs to activate heterotrimeric G proteins (3–6). Thus, pathway activation relies upon increasing the transition rate from the *off* state to the *on* state. There are no GPCRs in plants and other bikonts; the nucleotide exchange occurs spontaneously, without requiring GEF activity (7–9). G proteins are kept in the *off* state by a repressor such as a GAP or some other protein that holds the self-activating G protein in its inactive state. In this scenario, the presence of a stimulus results in derepression, i.e., removal of the repressing activity (10–12). Concerted activation and dererpression occur in the GTPase cycle of the yeast mating-response pathway (13, 14), in which the inactive GPCRs recruit a GAP protein and act to repress, whereas active receptors have GEF activity and act to activate. Thus, perception of a stimulus leads to concerted activation and derepression by increasing GEF activity while decreasing GAP activity.

These three mechanisms of signaling through molecular switches also occur in many other systems. For example, the activation mechanism described here is a simpler abstraction of a linear signaling cascade, a classical framework used to study general properties of signaling pathways (15–19), as well as to

Significance

Molecular switches are key components of intracellular signal-transduction pathways. Experimental work has established that the activity of molecular switches is regulated by three distinct mechanisms: 1) activation, 2) derepression, and 3) concerted (activation and derepression). However, it remains unclear how the choice of signaling mechanism influences the performance properties of the switch. Here, we characterize each switch design in terms of dose–response relationship, response time, and abilities to process upstream fluctuations. Our results highlight unique features of each mechanism and provide insight into the operating principles that underlie many different signaling pathways.

Author contributions: K.R.G., A.M.J., and T.C.E. designed research; K.R.G. and R.D.J. performed research; K.R.G. and R.D.J. contributed new reagents/analytic tools; K.R.G., R.D.J., A.M.J., and T.C.E. analyzed data; and K.R.G., A.M.J., and T.C.E. wrote the paper.

The authors declare no competing interest.

This article is a PNAS Direct Submission. J.H. is a guest editor invited by the Editorial Board.

[1]To whom correspondence may be addressed. Email: telston@med.unc.edu or alan_jones@unc.edu.

This article contains supporting information online at https://www.pnas.org/lookup/suppl/doi:10.1073/pnas.2013401118/-/DCSupplemental.

Published March 9, 2021.

model specific signaling pathways (20–22). While derepression may seem like an unusual mechanism, it occurs in numerous important signaling pathways in plants (e.g., auxin, ethylene, gibberellin, and phytochrome), as well as gene regulation (23–27). In many of these cases, derepression occurs through a decrease in the degradation rate of a component instead of its deactivation rate. Concerted mechanisms are found in bacterial two-component systems, wherein the same component acts as kinase and phosphatase (28–35).

Many previous studies have focused on the properties of a single switch mechanism without drawing comparisons between the three potential ways for initiating signaling. For example, the classical Goldbeter–Koshland model studied zero-order ultrasensitivity of an activation mechanism (15). Further analyses examined the effect of receptor numbers (36–38), feedback mechanisms (39, 40), and removal of active receptors via endocytosis and degradation (41, 42). Similarly, important properties of the concerted mechanism have been elucidated, such as its ability to perform ratiometric signaling (13, 14), to align dose responses at different stages of the signaling pathway (43), as well as its robustness (29, 44). The derepression mechanism is relatively less studied. Although there are models of G-signaling in *Arabidopsis thaliana* (45–47), these models have a large number of states and parameters and do not specifically examine distinct behaviors conferred by derepression.

What are the evolutionary constraints that may favor activation over derepression and vice versa? Seminal studies have investigated this question for gene-regulatory networks (48–50). However, an analysis of differences in the functional characteristics of activation, derepression, and concerted mechanisms in the context of cell signaling is still lacking. To address this deficiency, we perform a systematic comparison of the three mechanisms using the following metrics: 1) dose–response, 2) response time, and 3) ability to suppress or filter stochastic fluctuations in upstream components. The rationale behind comparing dose–response curves is that they provide information about the input sensitivity range and the output dynamic range, both of which are of pharmacological importance. We supplement this comparison with response times, which provide information about the dynamics of the signaling activity. The third metric of comparison is motivated from the fact that signaling pathways are subject to intrinsic fluctuations that occur due to the stochastic nature of biochemical reactions (51–56).

We construct and analyze both deterministic ordinary differential equation (ODE) models and stochastic models based on continuous-time Markov chains. We show that activation has the following two effects: It makes the switch response more sensitive than that of the receptor, and it speeds up the response with the stimulus strength. In contrast, derepression makes the switch response less sensitive than the receptor occupancy and slows down the response speed as stimulus strength increases. These counteracting behaviors of activation and derepression lead to intermediate sensitivity and intermediate response time for the concerted mechanism. In the special case of a perfect concerted mechanism (equal activation and repression), the dose–response curve of the pathway aligns with the receptor occupancy, and the response time does not depend upon the stimulus level. The noise comparison reveals that the concerted mechanism is more susceptible to fluctuations than the activation and derepression mechanisms, which perform similarly. We further show that these results qualitatively hold for more complex models, such as those incorporating receptor removal and proofreading. We finally discuss our findings to suggest reasons that might have led biological systems to evolve one of these mechanisms over the others, a question that has received considerable attention in the context of gene regulation (48–50).

Model Formulation

We consider a two-tier model for each of three mechanisms of signaling through a molecular switch (Fig. 1). The first tier is common for all mechanisms, where an inactive receptor (X) becomes active (X^*) when its corresponding input (stimulus) is presented. The second tier is the molecular switch that transitions between *off* (Y) and *on* (Y^*) states. In the activation mechanism, the transition rate from the *off* state to the *on* state increases as the number of active receptor molecules increases (Fig. 1*A*). In the derepression mechanism, the transition rate from the *on* state to the *off* decreases with a decrease in the number of inactive receptor molecules (Fig. 1*B*). In the concerted mechanism, both activation and derepression occur simultaneously (Fig. 1*C*). We model these mechanisms using ODEs, assuming mass-action kinetics. To this end, we denote the time by t, the stimulus level by S, the total number of receptors by X_T, and the total number of switches by Y_T. We use X^* and Y^* to denote the number of active receptors and the number of active switches, respectively. The rate constants are as follows: k_1 is the rate of receptor activation per unit stimulus, k_2 is the rate of receptor deactivation, k_3 is the basal rate of activation of the switch, k_4 is the basal rate of deactivation of the switch, k_5 is the strength of activation of an individual active receptor, and k_6 is the strength of repression of an individual inactive receptor. Thus, the (total) activation strength is $k_5 X_T$, and the (total) repression strength is $k_6 X_T$. Lastly, we assume that X_T and Y_T are conserved and that each model is in steady state before presentation of the stimulus at $t = 0$.

Note that the concerted mechanism encompasses both activation and derepression. Therefore, writing ODEs for the concerted mechanism is sufficient to capture all three mechanisms. The number of active receptors and the number of active switches evolve over time according to the following ODEs (*SI Appendix*, section S1):

$$\frac{dX^*}{dt} = k_1 S X_T - (k_1 S + k_2) X^*, \qquad \textbf{[1a]}$$

$$\frac{dY^*}{dt} = k_3 Y_T + k_5 Y_T X^* - (k_3 + k_4 + k_6 X_T) Y^* - (k_5 - k_6) X^* Y^*. \qquad \textbf{[1b]}$$

The activation and derepression mechanisms represent limiting cases in which $k_6 = 0$ and $k_5 = 0$, respectively. Solving Eq. **1** requires rate constants and initial conditions to be specified.

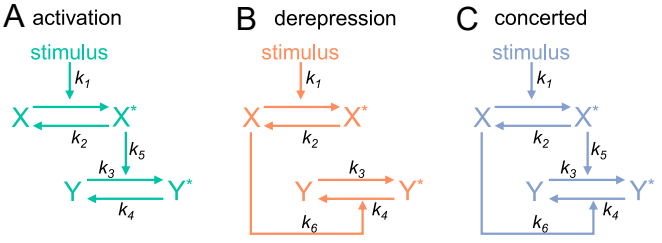

Fig. 1. Mechanisms for signaling through molecular switches. Presentation of a stimulus activates a receptor ($X \rightarrow X^*$). The reverse reaction causes deactivation of the receptor ($X^* \rightarrow X$). These transitions govern the activity of a molecular switch downstream. (*A*) In the activation mechanism, X^* increases the rate at which the inactive switch (Y) becomes active (Y^*). The opposite reaction $Y^* \rightarrow Y$ has a constant rate. (*B*) In the derepression mechanism, the transition $Y \rightarrow Y^*$ occurs at a constant rate. Activity of the switch is controlled through X: The stimulus decreases X and consequently increases Y^*. (*C*) In the concerted paradigm, both activation and derepression simultaneously control the downstream component.

We assume that initial conditions are given by the prestimulus ($S=0$) steady state:

$$X_0^* = 0, \quad Y_0^* = \frac{k_3}{k_3 + k_4 + k_6 X_T} Y_T. \qquad \textbf{[1c]}$$

With the models described by Eq. **1**, we next compare the three signaling mechanisms in terms of their dose responses and response times.

Dose Responses

We begin our analysis by examining the steady-state dose responses of activation, derepression, and concerted mechanisms. The steady-state solution to Eq. **1** is

$$\overline{X^*} = \frac{S X_T}{S + \frac{k_2}{k_1}}, \qquad \textbf{[2a]}$$

$$\overline{Y^*} = \frac{\frac{k_2 k_3}{k_1(k_3+k_4+k_5 X_T)} + \frac{k_3 + k_5 X_T}{k_3+k_4+k_5 X_T} S}{\frac{k_2(k_3+k_4+k_6 X_T)}{k_1(k_3+k_4+k_5 X_T)} + S} Y_T, \qquad \textbf{[2a]}$$

where $\overline{X^*}$ and $\overline{Y^*}$ represent the steady states for the number of active (occupied) receptors and the number of active switches, respectively. Notably, both $\overline{X^*}$ and $\overline{Y^*}$ have the form

$$R = \frac{R_0 \Theta_R + R_\infty S}{\Theta_R + S}, \qquad \textbf{[3]}$$

where R_0 is the minimum response corresponding to $S=0$, R_∞ is the maximum response corresponding to $S \gg \Theta_R$, and Θ_R is the stimulus concentration that produces half-maximal response $\frac{R_0+R_\infty}{2}$. The dynamic range of the response is given by $R_\infty - R_0$, signifying the maximum the output can change in response to the input. Eq. **3** shows that shapes of dose–response curves are the same for the three signaling mechanisms. Hence, comparison between them can be carried out in terms of R_0, R_∞, and Θ_R.

At the receptor level, $X_0^* = 0$ and $X_\infty^* = X_T$. The ratio $\frac{k_2}{k_1}$, which equals the binding affinity of the stimulus with the receptor, determines the half-maximal stimulus ($\Theta_{X^*} = \frac{k_2}{k_1}$) and the fractional receptor occupancy ($\frac{X}{X_T} = \frac{k_1 S/k_2}{1+k_1 S/k_2}$). For the switch, the response ($\overline{Y^*}$) is specified by:

$$Y_0^* = \frac{k_3 Y_T}{k_3 + k_4 + k_6 X_T}, \qquad \textbf{[4a]}$$

$$Y_\infty^* = \frac{(k_3 + k_5 X_T) Y_T}{k_3 + k_4 + k_5 X_T}, \qquad \textbf{[4b]}$$

$$\Theta_{Y^*} = \Theta_{X^*} \frac{k_3 + k_4 + k_6 X_T}{k_3 + k_4 + k_5 X_T}. \qquad \textbf{[4c]}$$

These expressions show that the dose–response of the switch depends upon the basal rates as well as activation strength ($k_5 X_T$) and repression strength ($k_6 X_T$). A careful examination of Eq. **4** provides the following insights:

1. The activation strength ($k_5 X_T$) does not affect the minimum response (Y_0^*), but affects the maximum response (Y_∞^*). In particular, increasing $k_5 X_T$ increases Y_∞^*. The repression strength ($k_6 X_T$) decreases Y_0^* and does not affect Y_∞^*.
2. Relative values of the repression and activation strengths dictate the relationship between the half-maximal stimulus for the switch response (Θ_{Y^*}) vis-á-vis the half-maximal stimulus for the receptor occupancy (Θ_{X^*}). More specifically, $\Theta_{Y^*} < \Theta_{X^*}$ when $k_5 X_T > k_6 X_T$, $\Theta_{Y^*} = \Theta_{X^*}$ when $k_5 X_T = k_6 X_T$, and $\Theta_{Y^*} > \Theta_{X^*}$ when $k_5 X_T < k_6 X_T$. Increasing $k_6 X_T$ increases Θ_{Y^*}, while increasing $k_5 X_T$ does the opposite.
3. The limiting case of $k_3 = 0$ implies $Y_0^* = 0$, and that of $k_4 = 0$ leads to $Y_0^* = Y_T$. Thus, nonzero basal rates reduce the dynamic range $Y_\infty^* - Y_0^*$ because $Y_\infty^* < Y_T$ and $Y_0^* > 0$. In the same vein, the relationship between Θ_{Y^*} and Θ_{X^*} is most sensitive to the ratio $k_6 X_T / k_5 X_T$ when $k_3 = 0$ and $k_4 = 0$.

Fig. 2 illustrates the features of the dose–response curves for the three mechanisms described above. For many signaling pathways, it is reasonable to assume negligible signaling activity in the absence of stimulus ($Y_0^* \ll Y_T$) and almost full activity for high stimulus levels ($Y_\infty^* \approx Y_T$). To meet these physiological constraints requires $k_3 \ll k_4 + k_6 X_T$ and $k_4 \ll k_3 + k_5 X_T$, respectively. Additionally, note that, for simplicity, we set basal rates equal to zero where possible. Thus, we use the following parameters for Fig. 2: $k_3 = 0$ and $k_6 = 0$ for activation; $k_4 = 0$

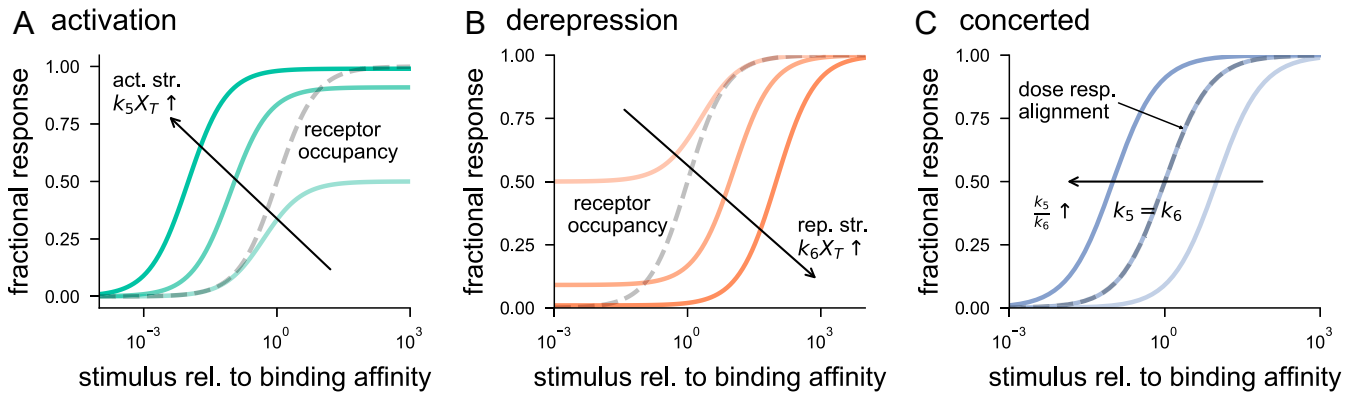

Fig. 2. Dose–response curves for signaling mechanisms through molecular switches. The response is measured in terms of fraction of active switches Y^*/Y_T as the stimulus level varies. The receptor-occupancy curve denotes the fraction of active receptors X^*/X_T. The stimulus is normalized by its binding affinity to the receptor (Θ_{X^*}). (*A*) For the activation mechanism, the half-maximal stimulus (Θ_{Y^*}) of a dose–response curve is less than Θ_{X^*}. Each dose–response curve (solid line) is for a fixed activation strength (act. str.) $k_5 X_T$. Increasing $k_5 X_T$, depicted by the solid arrow, causes an upward expansion and leftward shift in dose–response. For these plots, the following values for parameters were used: $k_3 = 0$, $k_4 = 1$ and $k_6 = 0$. The activation strength ($k_5 X_T$) was varied to take values from (1, 10, 100). (*B*) For the derepression mechanism, the dose–response of the switch for a given repression strength (rep. str.) ($k_6 X_T$) has half-maximal stimulus (Θ_Y) greater than Θ_{X^*}. Increasing $k_6 X_T$, shown by the solid arrow, leads to a downward expansion and rightward shift in the dose–response curve. The repression strength $k_6 X_T$ takes values from (1, 10, 100). The rest of the parameters were set as $k_3 = 1$, $k_4 = 0$, and $k_5 = 0$. (*C*) In the case of concerted mechanism, Θ_{Y^*} may be greater than, equal to, or less than Θ_{X^*}, depending upon the relative (rel.) values of the activation strength and the derepression strength. Increasing the ratio k_5/k_6, depicted by the solid arrow, shifts the dose response (resp.) to the left. Dose–response alignment ($\Theta_{Y^*} = \Theta_{X^*}$) occurs when $k_5 = k_6$. The parameters used for the plots are $k_3 = 0$ and $k_4 = 0$. The ratio k_5/k_6 was varied over (0.1, 1, 10).

and $k_5 = 0$ for derepression; and $k_3 = 0$ and $k_4 = 0$ for concerted. As shown in Fig. 2*A*, activation makes the switch response more sensitive to stimulus than the receptor occupancy ($\Theta_{Y^*} < \Theta_{X^*}$). Increasing the activation strength ($k_5 X_T$) increases Y^*_∞ and decreases Θ_{Y^*}, increasing the dynamic range (vertical expansion) and sensitivity (leftward shift) of the dose–response curve. The derepression mechanism exhibits an opposite behavior with $\Theta_{Y^*} > \Theta_{X^*}$. In this scenario, increasing the repression strength increases the dynamic range by decreasing Y^*_0 and decreases sensitivity by increasing Θ_{Y^*} (Fig. 2*B*).

Because we ignore the basal rates, changing activation and derepression strengths only influence Θ_{Y^*} in the case of a concerted mechanism. As expected, the switch response is more (less) sensitive than the receptor occupancy if activation (derepression) dominates derepression (activation). There is a perfect alignment of the fractional receptor-occupancy curve with the dose–response curve of the switch when $k_5 = k_6$ (Fig. 2*C*). Another important property of the concerted model is that it exhibits ratiometric signaling, in which the response of the switch (Y^*) is determined by the ratio of active receptors to the total number of receptors (X^*/X_T) (13, 14). The absolute value of the total number of receptors (X_T) has no bearing on $\overline{Y^*}$. This may be seen by setting $k_3 = 0$ and $k_4 = 0$ in the expression of $\overline{Y^*}$ in Eq. **2**:

$$\overline{Y^*} = \frac{S Y_T}{S + \frac{k_2 k_6}{k_1 k_5}}. \qquad [5]$$

In reality, k_3 and k_4 are likely to be small, but nonzero. Therefore, ratiometric signaling does not hold in a strict sense.

Our theoretical results above show how the dose–response curves behave differently for activation, derepression, and concerted mechanisms. Are some of these behaviors observed in biological systems? One example where the signaling response becomes maximal when only a small fraction of receptors are bound ($\Theta_{Y^*} < \Theta_{X^*}$) is the EGFR–MAPK pathway, which elicits a full MAPK response at less than 5% receptor occupancy (57). Our analysis explains this by an activation mechanism or a concerted mechanism, in which the activation strength dominates the repression strength. A contrasting behavior is seen in the ethylene pathway of *A. thaliana*, in which a loss-of-function mutation of one of the ethylene receptors, *etr1*, shows increased sensitivity to etylene (58). This points to a derepression mechanism in which the decreased amount of the receptor (X_T) lowers the repression strength $k_6 X_T$ and shifts the dose–response curve to the left in comparison to that of the wild-type system. A suggested example of concerted mechanism is the yeast G-signaling pathway, which exhibits both ratiometric signaling (13, 14) and dose–response alignment (43).

Response Times

Our analysis thus far focused on the steady-state properties of the activation, derepression, and concerted mechanisms. In this section, we study these mechanisms in terms of their response times; that is, the time it takes for a signaling output to reach its steady state. We use the following definition of response time:

$$\mathcal{T}_R = \frac{\int_0^\infty t \left|\overline{R} - R(t)\right| dt}{\int_0^\infty \left|\overline{R} - R(t)\right| dt}, \qquad [6]$$

where $R(t)$ is the time-dependent response of the pathway component under consideration and $\overline{R}$ represents its value at steady state (59). For this definition, $\mathcal{T}_R$ represents the "center of mass" of the response $R(t)$ and is well-defined when $R(0) \neq \overline{R}$. We may also think of $1/\mathcal{T}_R$ as the speed of the response in the sense that if the response is determined by a single kinetic step, $\mathcal{T}_R$ is the reciprocal of the rate constant for that step. For example, the response time for the receptor is given by (*SI Appendix*, section S2):

$$\mathcal{T}_{X^*} = \frac{1}{k_1 S + k_2}. \qquad [7]$$

Thus, the response time decreases (i.e., response speeds up) if $k_1 S + k_2$ increases. Because the response time depends upon the sum $k_1 S + k_2$ and the steady-state receptor occupancy depends upon the ratio $k_1 S / k_2$, these quantities can be tuned independently.

In the absence of stimulus, the response time of the switch follows the same form as Eq. **7**:

$$\mathcal{T}_{Y^*}|_{S=0} = \frac{1}{k_3 + k_4 + k_6 X_T}. \qquad [8]$$

When the stimulus is present, analytic solutions to the integrals in Eq. **6** for the response time of $Y^*(t)$ do not exist, except for a special case of the perfect concerted model $k_5 = k_6$. It is, however, possible to approximate $\mathcal{T}_{Y^*}$ by linearizing the ODE system in Eq. **1** around its steady state:

$$\mathcal{T}_{Y^*} \approx \underbrace{\frac{1}{k_3 + k_4 + k_6 X_T + (k_5 - k_6)\frac{k_1 S X_T}{k_1 S + k2}}}_{\text{resp. time of } Y^* \text{ when } X^* \text{is in steady-state}} + \underbrace{\frac{1}{k_1 S + k_2}}_{\text{resp. time of } X^*} \times \underbrace{\frac{k_3 + k_4 + k_6 X_T + (k_5 - k_6)\frac{k_1 S X_T}{k_1 S + k2}}{k_1 S + k_2 + k_3 + k_4 + k_6 X_T + (k_5 - k_6)\frac{k_1 S X_T}{k_1 S + k2}}}_{\text{time-averaging}}. \qquad [9]$$

This equation is exact for the special case when $k_5 = k_6$ (*SI Appendix*, section S3*C*). The first term in Eq. **9** can be interpreted as the response time of the switch when the receptors are at steady state, because in that case, the switch would be turned *on* at a rate $k_3 + k_5 \frac{k_1 S X_T}{k_1 S + k_2}$ and turned *off* at a rate $k_4 + k_6 X_T - k_6 \frac{k_1 S X_T}{k_1 S + k_2}$; so, the inverse of their sum would give the response time. The second term represents the response time of the receptor ($\mathcal{T}_{X^*}$) multiplied by a time-averaging factor, which computes the ratio of $\mathcal{T}_{X^*}$ to the sum of $\mathcal{T}_{X^*}$ and the response time of the switch when $X^* = \overline{X^*}$. The time-averaging term lies between zero and one; its value approaches zero if the receptor response is much faster than the switch response when $X^* = \overline{X^*}$ and approaches one if the receptor response is much slower than that of the switch.

If the receptor response is much faster than that of the switch, we expect that the latter does not depend upon the former (time-averaging term $\to 0$). Indeed, in this limit, Eq. **9** gives

$$\mathcal{T}_{Y^*} \approx \frac{1}{k_3 + k_4 + k_6 X_T + (k_5 - k_6)\frac{k_1 S X_T}{k_1 S + k2}}. \qquad [10]$$

Comparing Eq. **10** with the basal response time in Eq. **8** shows that for a given stimulus level, activation speeds up the response in comparison with the basal response. In contrast, derepression slows down the response, and a perfect concerted mechanism does not affect the response time (Fig. 3*A*). In the other limiting case, when the receptor timescale is much slower than that of the switch, we expect the receptor dynamics to dictate the response time (time-averaging term $\to 1$). Indeed, in this case, Eq. **9** reduces to $\mathcal{T}_{Y^*} \approx \mathcal{T}_{X^*}$, such that choice of the mechanism to control the switch has little effect on the response time. Our analytical as well as numerical calculations confirm this behavior (Fig. 3*A*).

An intuitive explanation for why activation is faster than derepression is as follows. Activation shortens the average lifetime of the *off* state, without affecting the average lifetime of the

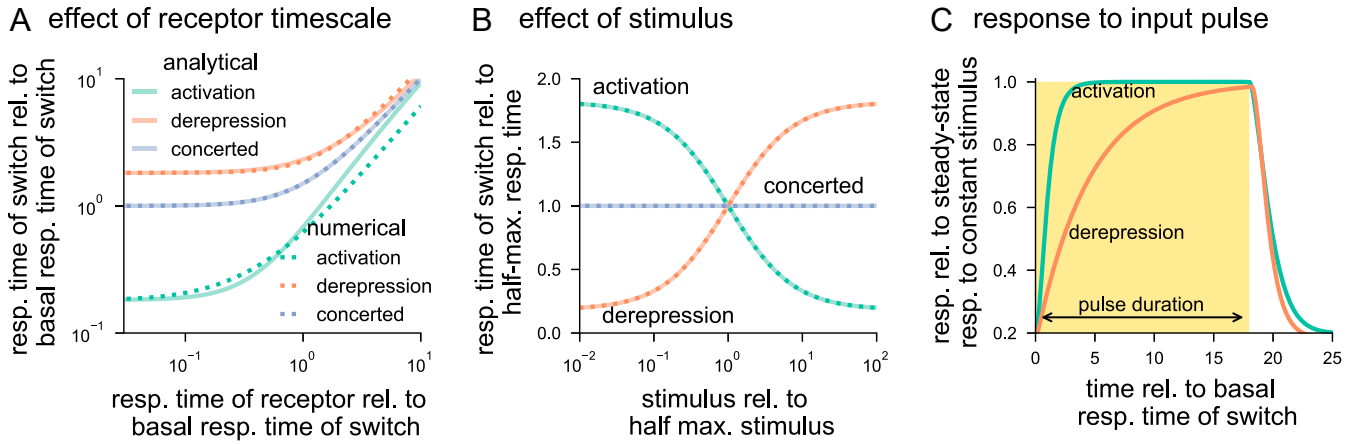

Fig. 3. Response times of molecular switches governed by activation, derepression, and concerted mechanisms. (*A*) The response (resp.) time of the switch increases as the response time of the receptor increases. Differences in the signaling mechanisms are more prominent when the receptor response is fast (i.e., the relative [rel.] response time of the receptor goes to zero). In this limit, activation decrease the response time, derepression increases the response time, and the concerted mechanism leaves it unchanged in comparison to the basal response time. For each signaling mechanism, the response time is computed by using the analytical result in Eq. **9** (solid lines) and numerically validated by using Eq. **6** (dashed lines). To ensure the same basal response and basal response time of the switches across signaling mechanisms, we chose the parameters as $k_3 = 1/9$, $k_4 = 1$, $k_6 = 0$, and $k_5 X_T = 10$ for activation; $k_3 = 1/9$, $k_4 = 0$, $k_5 = 0$, and $k_6 X_T = 1$ for derepression; and $k_3 = 1/9$, $k_4 = 0$, and $k_5 X_T = k_6 X_T = 1$ for concerted. The receptor response time was $k_1 S + k_2$ varied through k_2, while maintaining $k_1 S/k_2 = 1$. (*B*) With increase in the stimulus level, response time decreases for activation, increases for derepression, and does not change for the concerted mechanism. The comparison is controlled by setting same response time at half-maximal (half-max.) stimulus Θ_{Y^*}. The following parameters were chosen to have same basal response, but different basal response times: $k_3 = 1$, $k_4 = 9$, $k_5 X_T = 90$, and $k_6 = 0$ for activation; $k_3 = 10$, $k_4 = 0$, $k_5 = 0$, and $k_6 X_T = 90$ for derepression; and $k_3 = 10$, $k_4 = 0$, and $k_5 X_T = k_6 X_T = 90$ for concerted. The receptor occupancy was varied by changing $k_1 S/k_2$ while maintaining the receptor response time $1/(k_1 S + k_2)$, which was chosen to be 100 times faster than the response time of the switches at their respective half-maximal stimulus levels. (*C*) Comparing the system's response to a pulse of stimulus provides a method for distinguishing mechanisms. The response time for activation (derepression) following exposure to stimulus is shorter (longer) than following removal of stimulus. The time series for each mechanism is normalized to its steady state in the presence of stimulus. We used parameters such that each mechanism has the same response time of the switch in the absence of the stimulus and the stimulus strength produced a half-maximal response. Specific values of parameters are: $k_1 = 1$, $k_2 = 1$, $X_T = 100$, and $Y_T = 100$ for both mechanisms; $k_3 = 1/9$, $k_4 = 1$, $k_5 = 0.1$, and $S = 0.1$ for activation; and $k_3 = 1/9$, $k_4 = 0$, $k_6 = 0.01$, and $S = 10$ for derepression.

on state. Derepression operates differently; it does not affect the average lifetime of the *off* state, but increases the lifetime of the *on* state. Thus, activation responds faster than derepression. The concerted mechanism simultaneously decreases the lifetime of the *off* state and increases the lifetime of the *on* state. Therefore, its response time lies between those of activation and derepression.

Next, we examine how the response time varies with stimulus level (S). Because changing the stimulus affects the response time of the receptor, which, in turn, affects the response time of the switch, we control for this effect by keeping $k_1 S + k_2$ constant. We find that activation shortens the response time (speeds up the response) with increasing stimulus levels, whereas derepression increases the response time (slows down the response) (Fig. 3*B*). Importantly, the response time of the concerted mechanism is independent of the stimulus strength and, therefore, able to respond rapidly over the whole range of stimulus levels. To better understand this behavior, consider the response time for the limiting case of fast receptor dynamics. Eq. **10** can be rewritten as

$$\mathcal{T}_{Y^*} \approx \frac{\frac{1}{k_3+k_4+k_6 X_T}\Theta_{Y^*} + \frac{1}{k_3+k_4+k_5 X_T} S}{S + \Theta_{Y^*}}, \qquad [11]$$

which changes from $\frac{1}{k_3+k_4+k_6 X_T}$ at $S = 0$ to $\frac{1}{k_3+k_4+k_5 X_T}$ as $S \to \infty$. The half-maximal stimulus Θ_{Y^*} is the same as defined in Eq. **4**. For the activation mechanism, $\frac{1}{k_3+k_4+k_6 X_T} > \frac{1}{k_3+k_4+k_5 X_T}$, so the response time decreases with stimulus. Moreover, $\frac{1}{k_3+k_4+k_6 X_T} < \frac{1}{k_3+k_4+k_5 X_T}$ for the derepression mechanism and $\frac{1}{k_3+k_4+k_6 X_T} = \frac{1}{k_3+k_4+k_5 X_T}$ for the perfect concerted mechanism. Therefore, the response time increases with the stimulus for the derepression mechanism and is independent of the stimulus for the concerted case. It is also worth pointing out that activation is faster than derepression only if the basal response times are equal. Therefore, to construct a switch that responds rapidly using derepression, it is necessary for the switch to undergo fast basal cycling (Fig. 3*B*).

Our analysis of dose–response properties for ratiometric signaling given in Eq. **5** reveals that this mechanism is independent of the total number of receptors X_T when the basal rates of the switch are zero ($k_3 = 0$ and $k_4 = 0$). Using these values in the expression for the response time in Eq. **9** demonstrates that this property does not hold for the response time. Specifically, the response time decreases with an increase in X_T (*SI Appendix*, section S3*E*).

Up to this point, we have assumed that the input signal is constant in time. However, cells are often faced with environmental conditions that change in time, and challenging signaling pathways with time-dependent inputs is a powerful experimental technique for revealing the network motifs that regulate these systems (60, 61). To investigate how molecular switches respond to dynamic inputs, we first considered how each mechanism responds to a single pulse of stimulus in the form of a square wave. Using a time-dependent signal of this form provides a technique for distinguishing the activation and derepression mechanisms (Fig. 3*C*). If the response time following exposure to the stimulus is shorter (longer) than the time for the system to relax once the stimulus is removed, then the switch is primarily controlled by activation (derepression). We also consider the responses of receptor as well as switch governed by either of the three mechanisms to periodic input signals consisting of sequences of square wave pulses with varying frequency. We find that these architectures filter high-frequency inputs (*SI Appendix*, section S5).

Table 1. Transitions and associated rates for the stochastic model

Reaction	Population update	Transition rate
$X \rightarrow X^*$	$X^* \mapsto X^* + 1$	$k_1 S(X_T - X^*)$
$X^* \rightarrow X$	$X^* \mapsto X^* - 1$	$k_2 X^*$
$Y \rightarrow Y^*$	$Y^* \mapsto Y^* + 1$	$(k_3 + k_5 X^*)(Y_T - Y^*)$
$Y^* \rightarrow Y$	$Y^* \mapsto Y^* - 1$	$(k_4 + k_6(X_T - X^*))Y^*$

Processing Upstream Fluctuations

The deterministic models used to compare the signaling mechanisms thus far ignore the stochastic nature of biochemical reactions, which becomes relevant when the abundance of receptor and switch proteins are small (51–56, 62, 63). Therefore, we formulate a stochastic model of the concerted mechanism and analyze the other two mechanisms as its special cases. Our model consists of four reactions: activation of receptor upon recognizing the stimulus, deactivation of receptor, *on*-to-*off* transition of the molecular switch, and *off*-to-*on* transition of the molecular switch. The stochastic model is characterized by the probabilistic nature of each reaction, and the discreteness of changes in population counts upon occurrence of a reaction, as tabulated in Table 1.

Our goal is to analyze the noise properties of activation, derepression, and concerted mechanisms. We quantify noise using coefficient of variation squared (CV^2), which is computed by normalizing the variance by mean^2 and is a dimensionless quantity. To this end, we use the ODEs that describe the time evolution of the first- and second-order moments and solve them in steady state to obtain the stationary moments (64–66) (*SI Appendix*, section S4*A*). In particular, moments for the number of active receptors (X^*) are given by

$$\langle X^* \rangle = \frac{k_1 S X_T}{k_1 S + k_2}, \quad CV^2_{X^*} = \frac{\langle X^{*2} \rangle - \langle X^* \rangle^2}{\langle X^* \rangle^2} = \frac{1}{X_T}\frac{k_2}{k_1 S}. \qquad [12]$$

Here, $\langle . \rangle$ denotes the expected value (average) of its argument. These moments correspond to a binomial distribution with parameters X_T and $\frac{k_1 S}{k_1 S + k_2}$ (*SI Appendix*, section S4*A*). The stochastic mean $\langle X^* \rangle$ is same as the steady-state value for X^* in the deterministic model in Eq. **1**. The coefficient of variation squared increases as the number of receptors (X_T) decreases. Therefore, the noise analysis is important when X_T is small. In addition, the noise decreases with the ratio $k_1 S/k_2$. Recall that $k_1 S/k_2$ is the stimulus level relative to the binding affinity. Thus, the noise diminishes when the stimulus level is much higher than the binding affinity.

Closed-form expressions for the moments are not available for Y^*, owing to the nonlinear term $X^* Y^*$ in reaction rates, except for the special case of a perfect concerted model ($k_5 = k_6$). We approximate the mean response and the noise by considering a linearized system around the steady state

$$\langle Y^* \rangle \approx \frac{k_3 + k_5 \frac{k_1 S}{k_1 S + k_2} X_T}{k_3 + k_4 + k_6 \frac{k_2}{k_1 S + k_2} X_T} Y_T, \qquad [13a]$$

$$CV^2_{Y^*} \approx \underbrace{\frac{1}{Y_T}\frac{k_4 + k_6 X_T \frac{k_2}{k_1 S + k_2}}{k_3 + k_5 X_T \frac{k_1 S}{k_1 S + k_2}}}_{\text{contribution from act./deact. of } Y^*} +$$

$$CV^2_{X^*} \times \underbrace{\frac{k_3 + k_4 + k_5 \frac{k_1 S X_T}{k_1 S + k_2} + k_6 \frac{k_2 X_T}{k_1 S + k_2}}{k_1 S + k_2 + k_3 + k_4 + k_5 \frac{k_1 S X_T}{k_1 S + k_2} + k_6 \frac{k_2 X_T}{k_1 S + k_2}}}_{\text{time-averaging}}$$

$$\times \underbrace{\frac{\left(\frac{k_1 S}{k_1 S + k_2}\right)^2 (k_4 k_5 X_T + k_6 X_T (k_3 + k_5 X_T))^2}{\left(k_3 + k_5 \frac{k_1 S X_T}{k_1 S + k_2}\right)^2 \left(k_3 + k_4 + k_5 \frac{k_1 S X_T}{k_1 S + k_2} + k_6 \frac{k_2 X_T}{k_1 S + k_2}\right)^2}}_{\text{coupling}}. \qquad [13b]$$

We validate these approximations using exact semianalytical approach based on ref. 67 (*SI Appendix*, section S4*D*). The formula for $CV^2_{Y^*}$ above is written in terms of various sources of noise, as previously done for gene-regulation models (68–70). Specifically, the noise in the signaling activity of the switch arises from two sources: activation/deactivation reactions of the switch, and noise in the number of active receptors ($CV^2_{X^*}$). The contribution from activation/deactivation of the switch in Eq. **13** has a similar form as $CV^2_{X^*}$ in Eq. **12**. Accordingly, the contribution of this term decreases with an increase in Y_T or increase in the ratio of the total activation rate $\left(k_3 + k_5 X_T \frac{k_1 S}{k_1 S + k_2}\right)$ with total deactivation rate $\left(k_4 + k_6 X_T \frac{k_2}{k_1 S + k_2}\right)$. This ratio increases if the activation strength increases or the repression strength decreases. The contribution of CV^2_X to $CV^2_{Y^*}$ is scaled by time-averaging and coupling terms. The time-averaging term is the same as that in Eq. **9**; it varies between zero and one, depending upon the relative timescales of the receptor and the switch. Thus, in the limiting case where receptor dynamics is very fast, the contribution from $CV^2_{X^*}$ to $CV^2_{Y^*}$ becomes negligible due to efficient time-averaging of fluctuations in X^*. The coupling term in Eq. **13** determines how strongly X^* affects Y^*. For example, this term is zero when the stimulus is absent ($S = 0$) or when both k_5 and k_6 are zero. In both these cases, the switch is decoupled from the receptor.

Next, we compare the noise properties of activation, derepression, and concerted mechanisms. To mathematically control the comparison, we assume that the receptor dynamics is same across the three strategies. In addition, we maintain the same average rate at which the switch turns *on* from the *off* state—i.e., $k_3 + k_5 \frac{k_1 S X_T}{k_1 S + k_2}$—and the same average rate at which the switch turns *off* from the *on* state—i.e., $k_4 + k_6 \frac{k_2 X_T}{k_1 S + k_2}$. These assumptions ensure that differences in the noise properties, if any, are solely due to the architecture of the molecular switch, and not dependent on the parameters. With this setup, we examine the effect of relative timescales (response times) of the receptor and the switch. We observe that in Eq. **13**, varying $k_1 S + k_2$ while maintaining $k_1 S/k_2$ only affects the time-averaging term; all other terms are not affected. As shown in Fig. 4*A*, the noise properties of these signaling mechanisms are similar when the receptor timescale is fast. This is expected because the dominant contribution in $CV^2_{Y^*}$ comes from its own activation and deactivation. However, when the receptor timescale is slower than that of the switch, the overall noise increases, regardless of the signaling mechanism, and the noise performance of the concerted mechanism becomes worse than the other two mechanisms.

The observation that activation and derepression both have similar noise and their concerted action has higher noise is surprising in light of our analyses of dose–response and response time. In terms of these properties, activation and derepression counteract to enable intermediate response for the concerted mechanism. Intuitively, the increase in fluctuations occurs because in the concerted mechanism, fluctuations in the upstream component affect both transitions $Y \rightarrow Y^*$ and $Y^* \rightarrow Y$. In the case of activation and derepression, however, only one of these transitions is coupled with the upstream component. As a result, the concerted mechanism performs worse in terms of noise. We further highlight this observation by varying the relative strengths of activation ($k_5 X_T$) and derepression ($k_6 X_T$) in

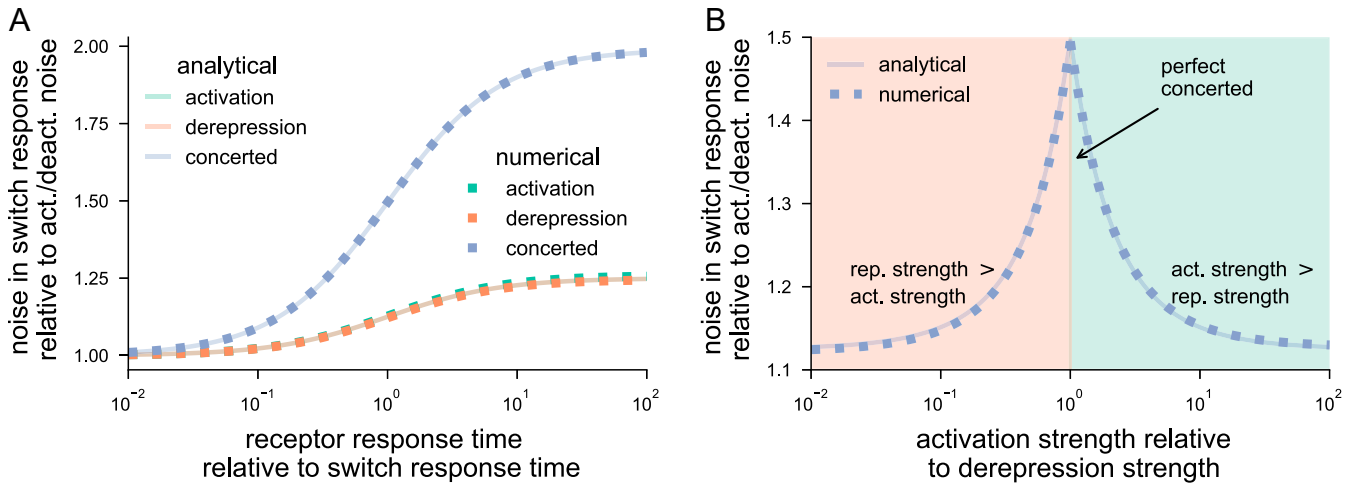

Fig. 4. Noise in the number of active switch molecules. Noise is quantified by using coefficient of variation squared ($CV^2_{Y^*}$) as in Eq. **13**. The overall $CV^2_{Y^*}$ is shown relative to the contribution from activation/deactivation (act./deact.) of Y^*. The analytical result is computed by using Eq. **13**, which is validated numerically. (*A*) Noise with change in response time of the receptor. The noise increases as receptor response time increases, i.e., as the receptor slows down in comparison with the switch response time. The concerted model has a higher noise than activation and derepression, which perform similarly. The difference is negligible when receptor dynamics is fast and is more prominent when receptor is slow. The receptor response time (k_1S+k_2) is varied by changing k_2, while keeping the same receptor occupancy through the ratio k_1S/k_2, so as to keep the same number of switches. The differences across signaling mechanisms are controlled by ensuring the same total activation rate of the switch $k_3+k_5\frac{k_1SX_T}{k_1S+k_2}$ and same total deactivation rate $k_4+k_6\frac{k_2SX_T}{k_1S+k_2}$. We used the following parameters: $k_3=0$, $k_4=1$, $k_5=0.02$, and $k_6=0$ for activation; $k_3=1$, $k_4=0$, $k_5=0$, and $k_6=0.02$ for derepression; and $k_3=0$, $k_4=0$, and $k_5=k_6=0.02$ for concerted. In addition, X_T and Y_T were taken to be 100 each. The receptor occupancy was maintained by $k_1S/k_2=1$. (*B*) Noise strength as a function of the relative (rel.) strengths of activation and derepression for a concerted mechanism. The noise is highest when the activation and derepression strengths match (perfect concerted mechanism). Deviating from the perfect concerted mechanism toward either stronger activation (shaded green region) or stronger derepression (shaded orange region) leads to smaller noise. Parameters were chosen such that total activation and the total deactivation rates were the same across signaling mechanisms. For derepression, the activation (act.) strength was kept constant, and the repression (rep.) strength k_6X_T was varied with a commensurate change in the basal deactivation rate k_4. For activation, the repression strength was kept constant, and the activation strength k_5X_T was increased with appropriate change in the basal activation rate k_3. We used the following parameters: $k_1=1$, $S=1$, $k_2=1$, $k_3+k_5\frac{k_1SX_T}{k_1S+k_2}=1$, $k_4+k_6\frac{k_2X_T}{k_1S+k_2}=1$, $X_T=100$, and $Y_T=100$.

Fig. 4*B*. The noise is greatest for the concerted mechanism when $k_5X_T=k_6X_T$.

We also analyze the special case of ratiometric signaling. Our deterministic analysis shows that for a concerted mechanism without basal rates ($k_3=0$ and $k_4=0$), the steady-state response ($\overline{Y^*}$) does not depend upon the total number of receptors (X_T). However, similar to the response time, the $CV^2_{Y^*}$ also depends upon X_T through the time-averaging term and $CV^2_{X^*}$, both of which decrease with increases in X_T (*SI Appendix*, section S4*B*). To summarize, ratiometric signaling only holds for the steady-state response. A cell that has higher X_T would respond faster as well as with less noise than a cell with a smaller X_T.

Model Generalizations

The two-tier models of signaling systems shown in Fig. 1 are purposely simplified for analytical tractability. In practice, signaling pathways comprise multiple tiers and frequently employ feedback regulation. Furthermore, one or more of the assumptions used to simplify the model equations are likely not to hold for any given pathway. Therefore, in this section, we examine how the models perform in more complicated situations.

Receptor Removal. The models shown in Fig. 1 assume conservation of receptor molecules (X_T) and switch molecules (Y_T). However, in many cases, ligated receptors are removed from the cell surface and subsequently degraded (42, 71–73). To account for this effect, we reformulated the models in Fig. 1 to include receptor production at a rate k_p, removal of inactive receptors with rate k_d, and removal of active receptors with rate k_d^*.

Inclusion of receptor removal results in the following modification of the ODE system in Eq. **1**:

$$\frac{dX}{dt}=k_p-k_dX-k_1SX+k_2X^*, \qquad \textbf{[14a]}$$

$$\frac{dX^*}{dt}=k_1SX-k_2X^*-k_d^*X^*, \qquad \textbf{[14b]}$$

$$\frac{dY^*}{dt}=(k_3+k_5X^*)(Y_T-Y^*)-(k_4+k_6X)Y^*. \qquad \textbf{[14c]}$$

The initial conditions are: $X(0)=\frac{k_p}{k_d}$, $X^*(0)=0$, and $Y^*(0)=\frac{k_3Y_T}{k_3+k_4+k_6k_p/k_d}$. As before, setting $k_6=0$ and $k_5=0$, respectively, results in ODEs for the activation and derepression mechanisms. When receptor production and removal are included in the model, the key qualitative differences between the activation and derepression mechanisms remain unchanged. For example, the functional forms of the dose–response curves are similar to those of Eq. **2** (*SI Appendix*, section S6). Some key features of the dose–response curves are:

1. The total number of receptors at steady-state $\overline{X}+\overline{X^*}$ remains k_p/k_d (prestimulus level) if $k_d=k_d^*$, becomes greater than k_p/k_d if $k_d>k_d^*$, and becomes less than k_p/k_d if $k_d<k_d^*$.
2. The half-maximal stimulus for the receptor response is $\Theta_X=\Theta_{X^*}=\frac{k_2+k_d^*}{k_1}\frac{k_d}{k_d^*}$, which now differs from the binding affinity of the receptor k_2/k_1.
3. The half-maximal stimulus for the switch response Θ_{Y^*} equals Θ_{X^*} if $k_6=k_5k_d/k_d^*$. Moreover, $\Theta_{Y^*}>\Theta_{X^*}$ if $k_6>k_5k_d/k_d^*$, and $\Theta_{Y^*}<\Theta_{X^*}$ if $k_6<k_5k_d/k_d^*$.

In terms of the response time, when the removal rates of inactive and active receptors are the same $k_d=k_d^*$, the response

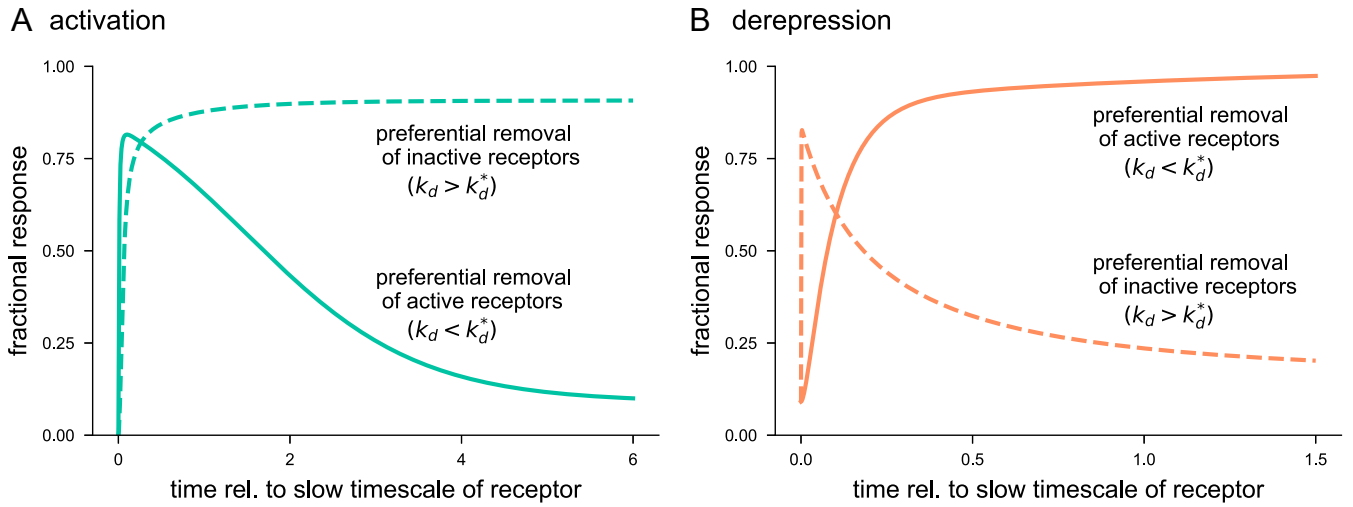

Fig. 5. Effect of receptor removal on responses of activation and derepression mechanisms. The response is measured in terms of fraction of active switch molecules (Y^*/Y_T) over time which is normalized to the slow timescale of the receptor (*SI Appendix*, section S6). (*A*) For an activation mechanism, the switch response adapts, i.e., returns toward basal response after a transient, if the rate of removal of active receptors (k_d^*) is higher than that of inactive receptors (k_d). In contrast, if inactive receptors are removed at a faster rate, then the response sustains. For the adaptive response, we chose $k_p = 0.11$, $k_d = 0.0011$, and $k_d^* = 0.11$. For the sustained response, we set $k_p = 101$, $k_d = 1.01$, and $k_d^* = 0.01$. The remaining parameters were selected as $k_1 = 1$, $k_2 = 1$, $k_3 = 0$, $k_4 = 10$, $k_5 = 1$, $k_6 = 0$, $S = 1$, and $Y_T = 100$. (*B*) For the derepression mechanism, preferential removal of X results in adaptation, whereas preferential removal of X^* causes sustained response. For the adaptive response, we used $k_p = 101$, $k_d = 1.01$, and $k_d^* = 0.01$. For the sustained response, we chose $k_p = 1$, $k_d = 0.01$, and $k_d^* = 1$. The remaining parameters were taken as $k_1 = 1$, $k_2 = 1$, $k_3 = 10$, $k_4 = 0$, $k_5 = 0$, $k_6 = 1$, $S = 100$, and $Y_T = 100$. Rel., relative.

time of Y^* is similar to that in Eq. **9**. As expected, activation speeds up the response, and derepression slows it down. However, when the receptor removal rates differ ($k_d \neq k_d^*$), then the expressions for response time become quite complicated (*SI Appendix*, section S6). In this case, a further assumption of fast receptor dynamics leads to the same conclusions for the three signaling mechanisms. As we discuss next, when the timescales of the receptor and switch are similar, more interesting behavior is possible.

Receptor removal has been shown to generate adaptive behavior in response to sustained stimulus. That is, the response is transient, eventually returning to near basal levels (74, 75). Our analysis revealed that if $k_d = k_d^*$, then both inactive receptors, $X(t)$, and active receptors, $X^*(t)$, monotonically approach their respective steady states. However, if $k_d \neq k_d^*$, then it is possible for $X(t)$ to transiently undershoot and for $X^*(t)$ to transiently overshoot steady state, producing an adaptive response. In particular, adaptation by $X^*(t)$ occurs when $k_d^* > k_d$, i.e., active receptors are removed at a faster rate than inactive receptors. In contrast, adaptation by $X(t)$ occurs when $k_d^* < k_d$ (*SI Appendix*, section S6*C*). If the kinetics of the switch is fast as compared to those of the receptor, the switch follows the transient changes in $X(t)$ and $X^*(t)$. Thus, for the activation mechanism to exhibit adaptive behavior requires that the active form of the receptor be preferentially removed ($k_d < k_d^*$) (Fig. 5*A*). Alternatively, for the derepression mechanism to exhibit an adaptive response requires the inactive form of the receptor to be preferentially removed ($k_d > k_d^*$) (Fig. 5*B*). For completeness, we examine the scenarios where the inactive receptors are preferentially removed for an activation mechanism and active receptors are preferentially removed for a derepression mechanism. Interestingly, in both these cases, the responses are sustained and do not adapt. These results thus provide another set of differences between activation and derepression mechanisms.

Kinetic Proofreading. Another simplification of the models shown in Fig. 1 is that the receptor kinetics is considered to be a single-step process. Recent work suggests that receptor kinetics is often more complex and may involve kinetic proofreading, in which a ligated receptor undergoes a series of transformations before becoming signaling competent (76–78). To study the effects of kinetic proofreading, we extend the model equations as follows:

$$\frac{dX_1^*}{dt} = k_1 S\left(X_T - \sum_{i=1}^{n} X_i^*\right) - (k_2 + k_f)X_1^*, \qquad \textbf{[15a]}$$

$$\frac{dX_i^*}{dt} = k_f X_{i-1}^* - (k_2 + k_f)X_i^*, \quad i = 2, 3, \ldots, N-1, \qquad \textbf{[15b]}$$

$$\frac{dX_N^*}{dt} = k_f X_{N-1}^* - k_2 X_N^*, \qquad \textbf{[15c]}$$

$$\frac{dY^*}{dt} = (k_3 + k_5 X_n^*)(Y_T - Y^*) - (k_4 + k_6 (X_T - X_n^*))\, Y^*. \qquad \textbf{[15d]}$$

Here, $n \geq 2$ is the total number of configurations for a ligated receptor, and k_f is the rate at which a ligated receptor transitions to the next configuration. We assume that all receptor states are capable of repressing the downstream switch, except X_n^*, which is the only competent state for activating the downstream switch (*SI Appendix*, section S7). Moreover, all receptors are assumed to be unligated before the arrival of the stimulus. Therefore, the initial conditions are $X_i^* = 0\,\forall i \in \{1, 2, \ldots, n\}$ and $Y^* = \frac{k_3 Y_T}{k_3 + k_4 + k_6 X_T}$.

Including multiple states for the receptor does not change the qualitative behavior of dose–response curves of the three signaling mechanisms. However, now, only a fraction of the total ligated receptors are signaling competent. This fraction is given by $(\frac{k_2}{k_2 + k_f})^{n-1}$ and depends on the rate at which a ligated receptor transitions toward the signaling-competent state, k_f, the rate of ligand release, k_2, and the number of configurations of the ligated receptors, n. The response time at the receptor level differs from that for the model in Fig. 1 and is given by

$$\mathcal{T}_{X_n^*} = \frac{1}{k_1 S + k_2} + \frac{1}{k_f + k_2} \frac{(n-1)(k_1 S + k_2)}{k_f + k_2 + (n-1)(k_1 S + k_2)}. \qquad \textbf{[16]}$$

Yet, the response time of the switch still has a similar decomposition as that in Eq. **9** (*SI Appendix*, section S7).

Cascades. Given that activation and derepression shift dose–response in opposite directions, a natural question to ask is whether dose–response alignment can occur in a signaling cascade where activation and derepression operate sequentially? To explore this possibility, we constructed a three-tier model where the response Y^* in Fig. 1*A* leads to derepression of a downstream component. Our analysis shows that, indeed, the dose response of the downstream component is better aligned with the receptor occupancy than the dose response of Y^* (*SI Appendix*, section S8). An alternate mechanism where derepression is followed by activation by modifying Fig. 1*B* also exhibits a similar behavior. For each of these cascades, as expected, the response time of the downstream component depends less strongly on the stimulus than that of Y^* (*SI Appendix*, section S8). It is worth noting that nonlinear regulation, such as feedback and feedforward loops, can also be used to compensate for undesirable characteristics of a given signaling mechanism. For example, negative feedback can align the dose–response curve with receptor occupancy for signaling pathways that operate through activation (43, 79, 80).

Having studied dose–response and response time of model generalizations, we next investigate the wider applicability of the results on the switch architectures' abilities to process upstream fluctuations. Instead of looking at specific generalizations, we assume that the inactive receptors $X(t)$ and the active receptors $X^*(t)$ are unspecified stochastic processes that are correlated with the number of active switches $Y^*(t)$. Specifically, we assume a positive correlation between $X^*(t)$ and $Y^*(t)$, and a negative correlation between $X(t)$ and $Y^*(t)$. This assumption is consistent with the models in Fig. 1 as well as models consisting of receptor removal and kinetic proofreading. We show that in such a setup, the steady-state noise in Y^* is highest for the concerted mechanism (*SI Appendix*, section S9). Thus, our findings on processing of upstream fluctuations by different signaling mechanisms are generalizable.

Discussion

Molecular switches are important components of most signaling pathways. Typically, these switches can exist in two states, *on* and *off*, and the presence of an external stimulus biases the switch toward the *on* state. This transition can occur either by increasing the *off*-to-*on* rate (activation), decreasing the *on*-to-*off* rate (derepression), or both (concerted). We characterized these three mechanisms in terms of their dose–response curves, response times, and abilities to process upstream fluctuations. We further examined how these three mechanisms were affected by some generalizations of the receptor dynamics. The following list summarizes key differences in the performance of switches based on activation, derepression, and concerted mechanisms:

- Both activation and derepression cannot align signaling activity with receptor occupancy. In particular, activation reduces the stimulus level required for half-maximal signaling as compared to 50% receptor occupancy ($\Theta_{Y^*} < \Theta_{X^*}$), whereas derepression produces a rightward shift of the dose–response curve ($\Theta_{Y^*} > \Theta_{X^*}$). The dose–response curve aligns with the receptor-occupancy curve ($\Theta_{Y^*} = \Theta_{X^*}$) for a perfect concerted mechanism (Fig. 2).
- A concerted mechanism is capable of ratiometric signaling, where the steady-state signaling output only depends upon fractional receptor occupancy, and not on the total number of receptors.
- The response time for the activation mechanism decreases with signal strength, whereas it increases for the derepression mechanism. Importantly, the response time for a perfect concerted mechanism is independent of signal strength (Fig. 3).
- Activation and derepression mechanisms respond similarly to upstream fluctuations, whereas the concerted mechanism is more susceptible to fluctuations (Fig. 4). Unlike the mean steady-state response, fluctuations in the output signal for the ratiometric signaling do depend on the total number of receptors.
- These results generalize to models that include more complex receptor dynamics, e.g., receptor removal and kinetic proofreading.
- Preferential removal of active (inactive) receptors leads to an adaptive response for the activation (derepression) mechanism and a sustained response for the derepression (activation) mechanism (Fig. 5).

These results suggest performance trade-offs in the operating characteristics for each mechanism. The activation mechanism can increase the sensitivity of the pathway and generate response times that decrease with signal strength, but at the cost of dose–response curves that do not align with receptor occupancy, potentially limiting the pathway's ability to transfer information (79). In this sense, the activation mechanism operates as an "eager" system that is sensitive to small receptor occupancy and accelerates the response for stronger signals. Therefore, activation seems appropriate for situations in which the cost of a false negative is greater than a false positive. For example, the adrenaline response to imminent danger should be sensitive and fast because cost of a false positive is small, but a false negative can be deadly.

Similar to the activation mechanism, derepression leads to misalignment of the dose–response curve and receptor occupancy. However, for derepression, the dose–response curve is shifted to the right. Another difference between these mechanisms is that for derepression, the response time increases with signal strength. Therefore, derepression acts as a "measured" system that does not respond to low receptor occupancy, waiting for a strong signal before committing to a response. Derepression seems appropriate for scenarios where the cost of a false positive is greater than a false negative. Interestingly, derepression-based signaling is found in many plants' pathways. We speculate that it happens because plants have to continually allocate their limited resources between growth in competition with their neighbors and immunity to survive pathogen attack (81, 82). For example, plants would perhaps ignore growth of a low level of pathogenic bacteria before allocating resources to fight them. Other possible scenarios where derepression may be used include irreversible cell-fate decisions such as the WNT pathway for embryo development (83) and fail-safe mechanisms such as the hypoxia-inducible factor in face of oxygen deprivation (84).

The concerted mechanism is better able to align with the receptor-occupancy curve than either the activation or derepression mechanisms. Therefore, it has better information fidelity (79). The concerted mechanism also can generate response times that are independent of the strength of the input signal. However, these features come at the cost of higher susceptibility to upstream fluctuations. We note that in a recent study, it was shown that ratiometric (concerted) signaling provided an advantage for gradient sensing, because it could compensate for spatial variations in the receptor concentration (14). The system under consideration in that study was the mating response of yeast. For this case, the spatial fluctuations in the receptor concentration were larger than downstream fluctuations in signaling, allowing the concerted mechanism to outperform an activation-based mechanism.

While misalignment of the dose–response curve with receptor occupancy can cause loss of information, it may also offer

some advantages. Consider a scenario where active receptors are preferentially removed, resulting in adaptation of the signaling response (Fig. 5). Recent work has shown that it is possible to exploit this feature to perform relative sensing (fold-change detection) if the receptor removal is a multistep process (42). Alternatively, a negative feedback may also result in an adaptive response and thereby a fold-change detection (59). A key feature of fold-change detection is that the sensitivity of the system decreases each time the system adapts (59, 85). Our results suggest that a relative sensing mechanism may be implemented with a derepression if the receptor removal operates on inactive receptors. We speculate that a negative feedback operating on inactive receptors would also yield the same effect.

Understanding the evolutionary constraints that favor either activation or derepression in the context of gene regulation is a long-standing question that has been addressed (48–50). Under the assumption that both mechanisms are functionally equivalent, these investigations theorized that activation is selected when demand for the gene product is high, whereas derepression is favored when demand is low. Our results reveal that these mechanisms have different operating characteristics. In particular, our analysis demonstrates that activation operates as an eager system and derepression as a measured system, thus providing a functional perspective when considering evolutionary advantages of each mechanism.

A limitation of our investigations is that the models we considered assumed mass-action kinetics for enzymatically driven reactions, and therefore do not capture saturation effects. While we do not anticipate that the qualitative features of our main results will change when this assumption is relaxed, it is possible that including saturation effects will produce behavior not captured by the current model. Therefore, extending our model to include saturation effects will be the subject of future investigations. Another future direction is to analyze the performance of the three switches when they are subjected to feedback and feedforward regulation. We end by noting that while we focused our investigations on signaling pathways, our results are likely to be relevant for understanding other intracellular systems, such as gene-regulatory networks and metabolic pathways.

Data Availability. Data have been deposited in GitHub (https://github.com/elstonlab/2021PNAS_SwitchComparison).

ACKNOWLEDGMENTS. We thank Daniel Lew (Duke University), Nicolas Buchler (North Carolina State University), Cesar A. Vargas-Garcia (Agrosavia), and members of the A.M.J. and T.C.E. laboratories for discussion and feedback. This work was supported by NSF Grant MCB–1713880 (to A.M.J. and T.C.E.) and NIH Grants R01 GM065989 (to A.M.J.) and R35 GM127145 (to T.C.E.).

1. F. R. Bischoff, H. Ponstingl, Catalysis of guanine nucleotide exchange on Ran by the mitotic regulator RCC1. *Nature* **354**, 80–82 (1991).
2. F. R. Bischoff, H. Krebber, T. Kempf, I. Hermes, H. Ponstingl, Human RanGTPase-activating protein RanGAP1 is a homologue of yeast Rna1p involved in mRNA processing and transport. *Proc. Natl. Acad. Sci. U.S.A.* **92**, 1749–1753 (1995).
3. N. Wettschureck, S. Offermanns, Mammalian G proteins and their cell type specific functions. *Physiol. Rev.* **85**, 1159–1204 (2005).
4. C. A. Johnston *et al.*, Structure of Gαi1 bound to a GDP-selective peptide provides insight into guanine nucleotide exchange. *Structure* **13**, 1069–1080 (2005).
5. D. P. Siderovski, F. S. Willard, The GAPs, GEFs, and GDIs of heterotrimeric G-protein alpha subunits. *Int. J. Biol. Sci.* **1**, 51 (2005).
6. W. M. Oldham, H. E. Hamm, Heterotrimeric G protein activation by G-protein-coupled receptors. *Nat. Rev. Mol. Cell Biol.* **9**, 60–71 (2008).
7. C. A. Johnston *et al.*, GTPase acceleration as the rate-limiting step in *Arabidopsis* G protein-coupled sugar signaling. *Proc. Natl. Acad. Sci. U.S.A.* **104**, 17317–17322 (2007).
8. J. C. Jones *et al.*, The crystal structure of a self-activating G protein α subunit reveals its distinct mechanism of signal initiation. *Sci. Signal.* **4**, ra8 (2011).
9. D. Urano *et al.*, G protein activation without a GEF in the plant kingdom. *PLoS Genet.* **8**, e1002756 (2012).
10. J. G. Chen *et al.*, A seven-transmembrane RGS protein that modulates plant cell proliferation. *Science* **301**, 1728–1731 (2003).
11. D. Urano *et al.*, Endocytosis of the seven-transmembrane RGS1 protein activates G-protein-coupled signalling in *Arabidopsis*. *Nat. Cell Biol.* **14**, 1079–1088 (2012).
12. X. Liang *et al.*, Ligand-triggered de-repression of *Arabidopsis* heterotrimeric G proteins coupled to immune receptor kinases. *Cell Res.* **28**, 529–543 (2018).
13. A. Bush *et al.*, Yeast GPCR signaling reflects the fraction of occupied receptors, not the number. *Mol. Syst. Biol.* **12** (2016).
14. N. T. Henderson *et al.*, Ratiometric GPCR signaling enables directional sensing in yeast. *PLoS Biol.* **17** (2019).
15. A. Goldbeter, D. E. Koshland, An amplified sensitivity arising from covalent modification in biological systems. *Proc. Natl. Acad. Sci. U.S.A.* **78**, 6840–6844 (1981).
16. R. Heinrich, B. G. Neel, T. A. Rapoport, Mathematical models of protein kinase signal transduction. *Mol. Cell* **9**, 957–970 (2002).
17. M. Chaves, E. D. Sontag, R. J. Dinerstein, Optimal length and signal amplification in weakly activated signal transduction cascades. *J. Phys. Chem. B* **108**, 15311–15320 (2004).
18. E. Feliu, M. Knudsen, L. N. Andersen, C. Wiuf, An algebraic approach to signaling cascades with n layers. *Bull. Math. Biol.* **74**, 45–72 (2012).
19. M. Beguerisse-Díaz, R. Desikan, M. Barahona, Linear models of activation cascades: Analytical solutions and coarse-graining of delayed signal transduction. *J. R. Soc. Interface* **13**, 20160409 (2016).
20. R. Macfarlane, An enzyme cascade in the blood clotting mechanism and its function as a biochemical amplifier. *Nature* **202**, 498–499 (1964).
21. C. Y. Huang, J. E. Ferrell, Ultrasensitivity in the mitogen-activated protein kinase cascade. *Proc. Natl. Acad. Sci. U.S.A.* **93**, 10078–10083 (1996).
22. B. N. Kholodenko, Cell-signalling dynamics in time and space. *Nat. Rev. Mol. Cell Biol.* **7**, 165–176 (2006).
23. V. Shingler, Signal sensing by σ54-dependent regulators: Derepression as a control mechanism. *Mol. Microbiol.* **19**, 409–416 (1996).
24. A. Dill, Tp. Sun, Synergistic derepression of gibberellin signaling by removing RGA and GAI function in *Arabidopsis thaliana*. *Genetics* **159**, 777–785 (2001).
25. L. E. Rogg, B. Bartel, Auxin signaling: Derepression through regulated proteolysis. *Dev. Cell* **1**, 595–604 (2001).
26. J. M. Alonso, A. N. Stepanova, The ethylene signaling pathway. *Science* **306**, 1513–1515 (2004).
27. K. M. Light, J. A. Wisniewski, W. A. Vinyard, M. T. Kieber-Emmons, Perception of the plant hormone ethylene: Known-knowns and known-unknowns. *J. Biol. Inorg. Chem.* **21**, 715–728 (2016).
28. F. D. Russo, T. J. Silhavy, The essential tension: Opposed reactions in bacterial two-component regulatory systems. *Trends Microbiol.* **1**, 306–310 (1993).
29. G. Shinar, R. Milo, M. R. Martínez, U. Alon, Input–output robustness in simple bacterial signaling systems. *Proc. Natl. Acad. Sci. U.S.A.* **104**, 19931–19935 (2007).
30. Y. Hart, Y. E. Antebi, A. E. Mayo, N. Friedman, U. Alon, Design principles of cell circuits with paradoxical components. *Proc. Natl. Acad. Sci. U.S.A.* **109**, 8346–8351 (2012).
31. Y. Hart, U. Alon, The utility of paradoxical components in biological circuits. *Mol. Cell* **49**, 213–221 (2013).
32. J. E. Ferrell, Jr, Feedback loops and reciprocal regulation: Recurring motifs in the systems biology of the cell cycle. *Curr. Opin. Cell Biol.* **25**, 676–686 (2013).
33. M. A. Rowland, E. J. Deeds, Crosstalk and the evolution of specificity in two-component signaling. *Proc. Natl. Acad. Sci. U.S.A.* **111**, 5550–5555 (2014).
34. B. N. Dubey *et al.*, Cyclic di-GMP mediates a histidine kinase/phosphatase switch by noncovalent domain cross-linking. *Science advances* **2**, e1600823 (2016).
35. L. Gelens, J. Qian, M. Bollen, A. T. Saurin, The importance of kinase–phosphatase integration: Lessons from mitosis. *Trends Cell Biol.* **28**, 6–21 (2018).
36. S. Strickland, J. N. Loeb, Obligatory separation of hormone binding and biological response curves in systems dependent upon secondary mediators of hormone action. *Proc. Natl. Acad. Sci. U.S.A.* **78**, 1366–1370 (1981).
37. A. Goldbeter, D. E. Koshland, Ultrasensitivity in biochemical systems controlled by covalent modification. Interplay between zero-order and multistep effects. *J. Biol. Chem.* **259**, 14441–14447 (1984).
38. J. E. Ferrell, Tripping the switch fantastic: How a protein kinase cascade can convert graded inputs into switch-like outputs. *Trends Biochem. Sci.* **21**, 460–466 (1996).
39. M. Behar, N. Hao, H. G. Dohlman, T. C. Elston, Mathematical and computational analysis of adaptation via feedback inhibition in signal transduction pathways. *Biophys. J.* **93**, 806–821 (2007).
40. M. Behar, N. Hao, H. G. Dohlman, T. C. Elston, Dose-to-duration encoding and signaling beyond saturation in intracellular signaling networks. *PLoS Comput. Biol.* **4** (2008).
41. V. Becker *et al.*, Covering a broad dynamic range: Information processing at the erythropoietin receptor. *Science* **328**, 1404–1408 (2010).
42. E. Lyashenko *et al.*, Receptor-based mechanism of relative sensing and cell memory in mammalian signaling networks. *eLife* **9**, e50342 (2020).
43. S. S. Andrews, W. J. Peria, C. Y. Richard, A. Colman-Lerner, R. Brent, Push-pull and feedback mechanisms can align signaling system outputs with inputs. *Cell Syst.* **3**, 444–455 (2016).
44. E. Batchelor, M. Goulian, Robustness and the cycle of phosphorylation and dephosphorylation in a two-component regulatory system. *Proc. Natl. Acad. Sci. U.S.A.* **100**, 691–696 (2003).

45. Y. Fu *et al.*, Reciprocal encoding of signal intensity and duration in a glucose-sensing circuit. *Cell* **156**, 1084–1095 (2014).
46. K. L. Liao *et al.*, A shadow detector for photosynthesis efficiency. *J. Theor. Biol.* **414**, 231–244 (2017).
47. K. L. Liao *et al.*, Dose-duration reciprocity for G protein activation: Modulation of kinase to substrate ratio alters cell signaling. *PloS One* **12** (2017).
48. M. A. Savageau, Design of molecular control mechanisms and the demand for gene expression. *Proc. Natl. Acad. Sci. U.S.A.* **74**, 5647–5651 (1977).
49. G. Shinar, E. Dekel, T. Tlusty, U. Alon, Rules for biological regulation based on error minimization. *Proc. Natl. Acad. Sci. U.S.A.* **103**, 3999–4004 (2006).
50. U. Gerland, T. Hwa, Evolutionary selection between alternative modes of gene regulation. *Proc. Natl. Acad. Sci. U.S.A.* **106**, 8841–8846 (2009).
51. Y. Sako, S. Minoghchi, T. Yanagida, Single-molecule imaging of EGFR signalling on the surface of living cells. *Nat. Cell Biol.* **2**, 168–172 (2000).
52. E. Korobkova, T. Emonet, J. M. Vilar, T. S. Shimizu, P. Cluzel, From molecular noise to behavioural variability in a single bacterium. *Nature* **428**, 574–578 (2004).
53. T. Shibata, K. Fujimoto, Noisy signal amplification in ultrasensitive signal transduction. *Proc. Natl. Acad. Sci. U.S.A.* **102**, 331–336 (2005).
54. M. Kaern, T. C. Elston, W. J. Blake, J. J. Collins, Stochasticity in gene expression: From theories to phenotypes. *Nat. Rev. Genet.* **6**, 451–464 (2005).
55. M. Ueda, T. Shibata, Stochastic signal processing and transduction in chemotactic response of eukaryotic cells. *Biophys. J.* **93**, 11–20 (2007).
56. J. Levine, H. Y. Kueh, L. Mirny, Intrinsic fluctuations, robustness, and tunability in signaling cycles. *Biophys. J.* **92**, 4473–4481 (2007).
57. T. Shi *et al.*, Conservation of protein abundance patterns reveals the regulatory architecture of the EGFR-MAPK pathway. *Sci. Signal.* **9**, rs6 (2016).
58. J. D. Cancel, P. B. Larsen, Loss-of-function mutations in the ethylene receptor ETR1 cause enhanced sensitivity and exaggerated response to ethylene in *Arabidopsis*. *Plant Physiology* **129**, 1557–1567 (2002).
59. M. Adler, P. Szekely, A. Mayo, U. Alon, Optimal regulatory circuit topologies for fold-change detection. *Cell Syst.* **4**, 171–181 (2017).
60. E. A. Davidson, A. S. Basu, T. S. Bayer, Programming microbes using pulse width modulation of optical signals. *J. Mol. Biol.* **425**, 4161–4166 (2013).
61. A. E. Pomeroy *et al.*, A predictive model of gene expression reveals the role of regulatory motifs in the mating response of yeast. *Sci. Signal.* **14**, eabb5235 (2021).
62. D. A. McQuarrie, Stochastic approach to chemical kinetics. *J. Appl. Probab.* **4**, 413–478 (1967).
63. C. V. Rao, D. M. Wolf, A. P. Arkin, Control, exploitation and tolerance of intracellular noise. *Nature* **420**, 231–237 (2002).
64. A. Singh, J. P. Hespanha, Stochastic hybrid systems for studying biochemical processes. *Phil. Trans. Math. Phys. Eng. Sci.* **368**, 4995–5011 (2010).
65. D. Schnoerr, G. Sanguinetti, R. Grima, Approximation and inference methods for stochastic biochemical kinetics—A tutorial review. *J. Phys. Math. Theor.* **50**, 093001 (2017).
66. K. R. Ghusinga, C. A. Vargas-Garcia, A. Lamperski, A. Singh, Exact lower and upper bounds on stationary moments in stochastic biochemical systems. *Phys. Biol.* **14**, 04LT01 (2017).
67. K. R. Ghusinga, A. Lamperski, A. Singh, Moment analysis of stochastic hybrid systems using semidefinite programming. *Automatica* **112**, 108634 (2020).
68. J. Paulsson, Summing up the noise in gene networks. *Nature* **427**, 415–418 (2004).
69. M. Komorowski, J. Miekisz, M. P. Stumpf, Decomposing noise in biochemical signaling systems highlights the role of protein degradation. *Biophys. J.* **104**, 1783–1793 (2013).
70. M. Soltani, C. A. Vargas-Garcia, D. Antunes, A. Singh, Intercellular variability in protein levels from stochastic expression and noisy cell cycle processes. *PLoS Comput. Biol.* **12** (2016).
71. S. S. Ferguson, Evolving concepts in G protein-coupled receptor endocytosis: The role in receptor desensitization and signaling. *Pharmacol. Rev.* **53**, 1–24 (2001).
72. J. M. Smith, D. J. Salamango, M. E. Leslie, C. A. Collins, A. Heese, Sensitivity to flg22 is modulated by ligand-induced degradation and de novo synthesis of the endogenous flagellin-receptor FLAGELLIN-SENSING2. *Plant Physiology* **164**, 440–454 (2014).
73. A. J. Guskjolen, Losing connections, losing memory: AMPA receptor endocytosis as a neurobiological mechanism of forgetting. *J. Neurosci.* **36**, 7559–7561 (2016).
74. W. Ma, A. Trusina, H. El-Samad, W. A. Lim, C. Tang, Defining network topologies that can achieve biochemical adaptation. *Cell* **138**, 760–773 (2009).
75. J. E. Ferrell, Jr, Perfect and near-perfect adaptation in cell signaling. *Cell Syst.* **2**, 62–67 (2016).
76. T. W. McKeithan, Kinetic proofreading in T-cell receptor signal transduction. *Proc. Natl. Acad. Sci. U.S.A.* **92**, 5042–5046 (1995).
77. O. S. Yousefi *et al.*, Optogenetic control shows that kinetic proofreading regulates the activity of the T cell receptor. *eLife* **8**, e42475 (2019).
78. D. K. Tischer, O. D. Weiner, Light-based tuning of ligand half-life supports kinetic proofreading model of T cell signaling. *eLife* **8**, e42498 (2019).
79. C. Y. Richard *et al.*, Negative feedback that improves information transmission in yeast signalling. *Nature* **456**, 755–761 (2008).
80. L. Yan, Q. Ouyang, H. Wang, Dose-response aligned circuits in signaling systems. *PloS One* **7** (2012).
81. B. Huot, J. Yao, B. L. Montgomery, S. Y. He, Growth–defense tradeoffs in plants: A balancing act to optimize fitness. *Mol. Plant* **7**, 1267–1287 (2014).
82. I. T. Major *et al.*, Regulation of growth–defense balance by the JASMONATE ZIM-DOMAIN (JAZ)-MYC transcriptional module. *New Phytol.* **215**, 1533–1547 (2017).
83. H. Clevers, R. Nusse, Wnt/β-catenin signaling and disease. *Cell* **149**, 1192–1205 (2012).
84. S. Salceda, J. Caro, Hypoxia-inducible factor 1α (HIF-1α) protein is rapidly degraded by the ubiquitin-proteasome system under normoxic conditions. *J. Biol. Chem.* **272**, 22642–22647 (1997).
85. N. Olsman, L. Goentoro, Allosteric proteins as logarithmic sensors. *Proc. Natl. Acad. Sci. U.S.A.* **113**, E4423–E4430 (2016).